Theoretical Analysis of Self-Starting Busemann Intake Family

N. Moradian, E. Timofeev, R. Tahir

Abstract—In this work, startability of the Busemann intake family with weak/strong conical shock, as most efficient intakes, via overboard mass spillage method is theoretically analyzed. Masterix and Candifix codes are used to numerically simulate few models of this type of intake and verify the theoretical results. Portions of the intake corresponding to various flow capture angles are considered to have mass spillage in the starting process of this intake. This approach allows for overboard mass spillage via a V-shaped slot with the tip of V coinciding with the focal point of the Busemann flow. The theoretical results, achieved using two different theories, of self-started Busemann takes with weak/strong conical shock show that significant improve in intake startability using overboard spillage technique. The starting phenomena of Busemann intakes with weak conical shock and seven different capture angles are numerically simulated at freestream Mach number of 3 to find the minimum area ratios of self-started intakes. The numerical results confirm the theoretical ones achieved by authors.

Keywords—Busemann intake, conical shock, overboard spillage, startability.

I. INTRODUCTION

THE scramjet air intake is essentially a converging duct decelerating and compressing airflow and supplying the compressed air to the engine's combustor. In order to minimize the pressure loss and have the most efficient compression, intake of air-breathing engine should be able to capture all incoming air, and a supersonic flow gets established throughout the intake at the design free-stream Mach number (i.e. intake should be started). In unstarted supersonic air intake, the flow inside the intake is subsonic after passing through a bow shock in front of the intake, and less airflow is captured with lower efficiency and pressure recovery [1]-[5]; thus, it is not suitable for the engine's operation.

By designing the intake with an appropriate area ratio (the ratio of the exit area to the entry area of the intake), it is possible to control the startability of the intake. In order to start the intake spontaneously, the isentropic intake's area ratio should be more than Kantrowitz limit which is defined by Kantrowitz and Donaldson [6] and Kantrowitz [7] to predict the flow starting or unstarting in converging ducts.

The Kantrowitz limit is determined by assuming a normal

N. Moradian was with McGill University, Montreal, Quebec H3A0C3, Canada. She is now working as self-dependent researcher (corresponding author, phone: 514-758-2660; e-mail: niloofar.moradian@mail.mcgill.ca).
E. Timofeev, is associate professor in Department of Mechanical Engineering, McGill University, Montreal, Quebec H3A0C3, Canada.(e-mail: evgeny.timofeev@mcgill.ca).
R. Tahir is with Etobicoke, Ontario, M9V 1X1, Canada. (e-mail: rabi.tahir@rogers.com).

shock at the intake entrance so that all incoming mass flow is captured by the intake. Then, the isentropic area ratio for the flow Mach number downstream of the shock represents the Kantrowitz limit of the intake area ratio. The intake area ratio must be equal or greater than the above limiting value for spontaneous intake starting. In Kantrowitz theory of fully enclosed intake, it is assumed that the flow downstream of the shock is quasi-one-dimensional, quasi-steady, and isentropic.

During last decades, designers try to use different methods to lower the Kantrowitz limit to self-start intakes much easier. Many methods such as overspeeding, variable geometry, mass spillage via wall perforations, etc. are used by them to reach this goal. Arguably the best method to improve the startability of an intake is overboard spillage technique. The overboard spillage technique relies for starting an intake on the overboard spillage of the incoming flow during the starting process by moving the cowl toward downstream. In an unstarted intake, the flow which cannot pass through the intake exit gets spilled from the cowl region. The spillage amount is decreased by moving the shock toward the cowl lip until the shock reaches the coal lip. Then, if the Kantrowitz limit is satisfied, the shock is swallowed and the intake becomes started.

Using overboard spillage technique to start different types of planar intakes is studied by Veillard et al. [8] and Sun and Zhang [9] theoretically and Hohn and Gulhan [10] experimentally investigated the improvement of planar intakes' startability using this technique. The outcomes of all these studies along with the numerical and analytical results of previous studies done by [11], [12] on startability analysis of Prandtl-Meyer intakes using overboard spillage technique, confirm the benefits of using this method to increase the startability of intakes. This improvement gets clearer from the study Rosli et al. [13] which showed that for low Mach numbers, overboard spillage increases startability up to 40% (in terms of area ratio). Thus, this technique is used as one of the best techniques to improve the startability of different type of intakes such as Busemann intake.

Busemann in 1929 [15] outlined the theoretical aspects of an axial, conically symmetric, supersonic flow called Busemann flow and, subsequently, Taylor and Maccoll [16] published the second order differential equation for this flow. Later on, Molder and Szpiro [14] presented the basics of Busemann intake design and highlighted some idiosyncrasies of Busemann flow as explained above. Molder [17] showed that a Busemann intake can reduce the Mach number from 8.33 to 2.8 with a total pressure recovery of 91%. The existence of Busemann flow in a Busemann intake was shown

World Academy of Science, Engineering and Technology
International Journal of Mechanical and Mechatronics Engineering
Vol:11, No:5, 2017

experimentally using flow visualization by Molder [18]. In this intake, isentropic compression in a conical flow deflects the incoming stream towards the axis of symmetry. Then, the conical shock returns the flow to its original direction, and the shock is canceled at the end of the intake wall surface to yield an axial, uniform outflow at a lower Mach number [14], [19]-[22], see Fig. 1.
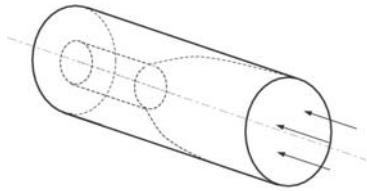

Fig. 1 Schematics of Busemann intake

In this study, the process of designing a Busemann intake, along with the suggestion way to introduce overboard spillage into Busemann intake design which is amenable to the analytical startability analysis, is explained. The theoretical approach to account for overboard spillage and predict spontaneous starting characteristics for Busemann intakes with overboard spillage is presented, and different designs of Busemann intakes are then studied from the point of view of achieving better starting characteristics. Similar to Veillard et al. in [8] and Moradian and Timofeev in [11], [12] studies on the startability of the whole family of two-shock ramp intakes and Prandtl-Meyer intakes with overboard spillage, it is of interest to find out whether the strong-shock-based design principle would hold for Busemann intakes as well.

II. BUSEMANN FLOW AND BUSEMANN INTAKE WITH OVERBOARD SPILLAGE

Busemann flow is an axisymmetric conical internal flow [19]. Its isentropic compression starts at the free-stream Mach angle and decelerates the flow from a high free-stream Mach number to a lower one. Busemann flow is a conical one with the focal point at the axis of symmetry (see Fig. 2). The compressed flow passes through a conical shock, resulting in an irrotational and uniform downstream flow parallel to the free-stream flow. In principle, the flow downstream of the conical shock may be subsonic or supersonic depending on whether the conical shock is strong or weak.

The Busemann intake is designed on the basis of Busemann flow. The isentropic compression of flow from the Mach cone to the shock cone is schematically shown in Fig. 2. The streamline of Busemann flow represents the Busemann intake's wall which can be obtained by integration of the Taylor-Maccoll and streamline equations with for example, a fourth order Runge-Kutta method [17]. The integration should be carried out starting from a chosen Mach number M_2 upstream of the conical shock with the aerodynamic shock angle θ_a (see Fig. 2) and proceeding in the upstream direction. The free-stream Mach number M_∞ and the intake's area ratio A_e/A_i result from the integration.
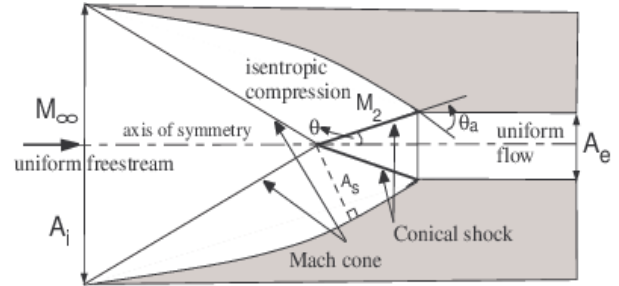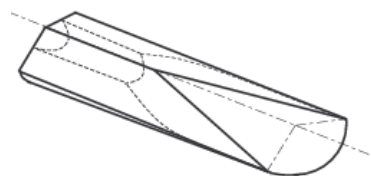

Fig. 2 Flowfield schematics in an axial cross-section of a fully enclosed, axisymmetrical, Busemann intake

The fully enclosed Busemann intake with high contraction (e.g., Fig. 2) is difficult to start. One of the ways to overcome this difficulty is to design an intake which would allow overboard spillage in the starting process while retaining the Busemann flowfield in the started mode.
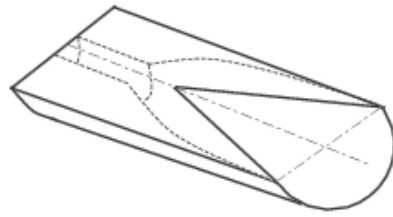
The first step to design Busemann intakes with overboard spillage is to select a portion of full axisymmetrical Busemann flow characterized by the central angle ϕ ranging from $0°$ to $360°$. The value of ϕ tending to $0°$ would result in a very thin slice of the original axisymmetrical Busemann flow, while the full axisymmetrical Busemann intake represents by ϕ equal to $360°$, see Fig. 1. Some intermediate cases with $\phi = 90°$, $\varphi = 180°$, and $\phi = 270°$ are respectively shown in Figs. 3 (a)-(c). The selected portion of the intake is bounded by two cutting planes intersecting at the axis of symmetry of Busemann flow. The angle between the planes is equal to ϕ (for $\phi \leq 180°$) or $360° - \phi$ (for $\phi \geq 180°$). For $\phi < 360°$, the flow capture area of the original full intake is reduced proportionally; therefore, the angle ϕ is therein to be called capture angle.

As the second step, each of the above-mentioned cutting planes is covered by a flat plate in order to: (a) provide some opening for overboard spillage; (b) ensure that in case of started flow, the intake flow would remain to be Busemann flow. Considering flat plates with the leading edges forming the Mach angle with the free-stream and extending from the leading edge of the intake to the focal point of the Busemann flow would satisfy the both two goals simultaneously.
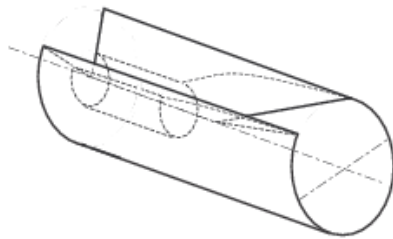
Clearly, as shown in Figs. 3 (a)-(c), the amount of spillage increases with decrease of the capture angle ϕ; however, the side view of the flowfields in the intakes with overboard spillage is the same for all angles $\phi < 360°$, see Fig. 3 (d). Therefore, it would be logical to expect better self-starting characteristics when $\phi \to 0$.
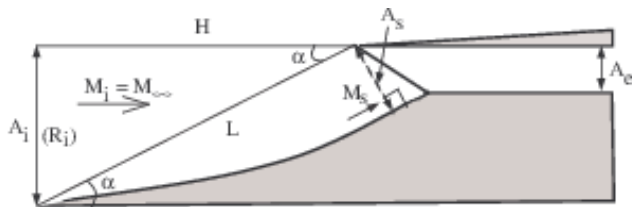

(a) 3D view; capture angle $\phi = 90°$

World Academy of Science, Engineering and Technology
International Journal of Mechanical and Mechatronics Engineering
Vol:11, No:5, 2017

(b) 3D view; capture angle $\phi = 180°$

(c) 3D view; capture angle $\phi = 270°$

(d)   Cross-sectional view; capture angle $\phi = 90°$

Fig. 3 Busemann intakes with overboard spillage

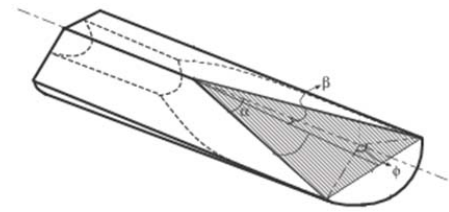*A. Spillage Calculation for Busemann Intakes with Different Capture Angles*

Busemann intakes can have different capture angles ϕ, from $0°$ to $\phi < 360°$. Decreasing the capture angle of the Busemann intake increases the magnitude of spillage amount. For subsequent determination of the self-starting area ratios of Busemann intakes with overboard spillage, it is necessary to evaluate the magnitude of mass spillage for various capture angles. In this study, the spillage amount is obtained from purely geometrical considerations on the basis of the magnitude of spillage area A_{spill} alone. Two different theories are suggested to evaluated A_{spill} for Busemann intakes with different capture angles. Furthermore, the maximum spillage area $A_{max-spill}$ for small capture angle $\phi \to 0$ is evaluated too within each theory.

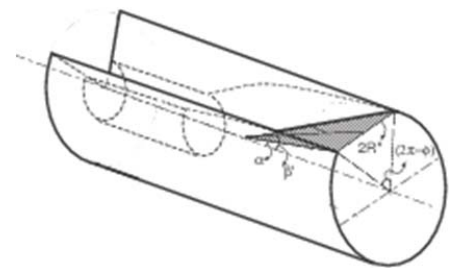1) AA) Theory I

The Busemann intakes are divided into two main categories based on their capture angles: I) $0° < \phi \leq 180°$: Busemann intakes with capture angles greater than zero and less than or equal to $180°$; II)$180° \leq \phi < 360°$: Busemann intakes with capture angles equal to or greater than $180°$ and less than $360°$.

In this theory, as shown in Fig. 4, for both categories the opening area of the external compression section represents the spillage area A_{spill}.

(a) $0° < \phi \leq 180°$

(b) $180° \leq \phi < 360°$

Fig. 4 Schematic representation of the spillage area in Busemann intakes (Theory I)

For Busemann intake in category (I), as can be easily deduced from Fig. 4 (a), the spillage area is equal to:

$$A_{spill-(\phi \leq 180°)} = \frac{R_i}{\tan \alpha \cos \beta}\left(R_i \sin\left(\frac{\phi}{2}\right)\right)$$
$$= \frac{R_i}{\tan \alpha \left(\tan \alpha \cos\left(\frac{\phi}{2}\right)\right)}\left(R_i \sin\left(\frac{\phi}{2}\right)\right) \quad (1)$$

where R_i is the radius of the inlet cross-section, and α is the Mach angle of the free-stream flow, and other notations are shown in Figs. 4 (a)and 3 (d).

For Busemann intake in category (II), as shown in Fig. 4 (b), the spillage area is equal to:

$$A_{spill-(\phi \geq 180°)} = \frac{R_i}{\tan \alpha \cos \beta'}\left(R_i \sin\left(\frac{\phi}{2}\right)\right)$$
$$= \frac{R_i}{\tan \alpha \left(-\tan \alpha \cos\left(\frac{\phi}{2}\right)\right)}\left(R_i \sin\left(\frac{\phi}{2}\right)\right) \quad (2)$$

The maximum spillage amount for a thin $\phi \to 0$ Busemann intake $A_{max-spill}$ is represented by the length of L, see the side view in Fig. 3 (d).

2) BB) Theory II}

In Theory II, the projections of the shaded areas in Fig. 4 to

World Academy of Science, Engineering and Technology
International Journal of Mechanical and Mechatronics Engineering
Vol:11, No:5, 2017

the horizontal plane are considered as the area which represents the spillage area, as illustrated in Fig. 5. In this case, when $\phi \to 0$, the maximum spillage area $A_{max-spill}$ can be represented by the length H (Fig. 3 (d)). The new spillage areas for Busemann intakes with different capture angles can be then found as (see Fig. 5 for details):

$$A_{spill-(\phi \leq 180°)} = A_{spill-(\phi \geq 180°)} = \frac{R_i}{\tan \alpha} \left(R_i \sin\left(\frac{\phi}{2}\right) \right) \qquad (3)$$

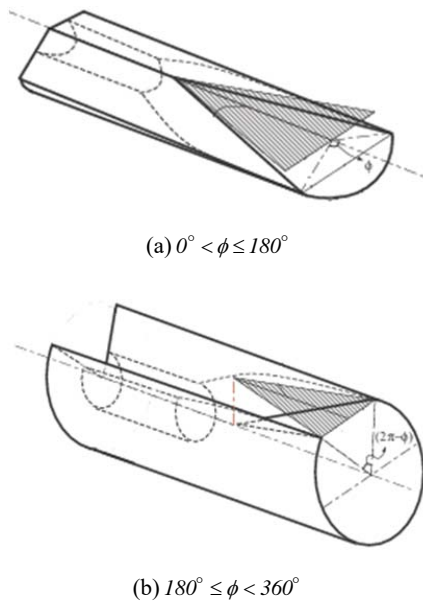(a) $0° < \phi \leq 180°$

(b) $180° \leq \phi < 360°$

Fig. 5 Schematic representation of the spillage area in Busemann intakes (Theory II)

It is obvious from (1)-(3) that the spillage area A_{spill} predicted by Theory I and Theory II tends to zero when the capture angle $\phi \to 0$. This is consistent with the fact that the inlet area $A_{(i-\phi)} = \left(R_i^2 / 2 \right) \phi$ tends to zero as well when $\phi \to 0$. To analyze the startability of the intake, the spillage area A_{spill} is to be normalized by the inlet area A_i. In this case, one would have the dependency on ϕ as $(\sin \phi/2)$ which tends to unity when $\phi \to 0$. Therefore, the ratio (A_{spill}/A_i) has a finite limit when $\phi \to 0$. The maximum spillage area $A_{max-spill}$ should be also normalized by the inlet area $A_{(i-0)}$ for every thin intake, which can be presented by the length R_i.

III. STARTING OF BUSEMANN INTAKES VIA OVERBOARD SPILLAGE

In order to follow Kantrowitz theory to determine the startability of fully enclosed Busemann intakes, a normal shock is placed at the entry cross-section of the intake. The flow gets subsonic downstream of the normal shock and accelerates isentropically towards the intake's exit. At the given free-stream Mach number, for the area ratios equal

orexceeding the exit-to-entry area ratioresulting in flow choking at the exit, the intake would start spontaneously. Calculating the limiting area ratios of started intakes for various free-stream Mach numbers results in the Kantrowitz line shown as a thin solid line on the area ratio/free-stream Mach number diagram in Fig. 6.
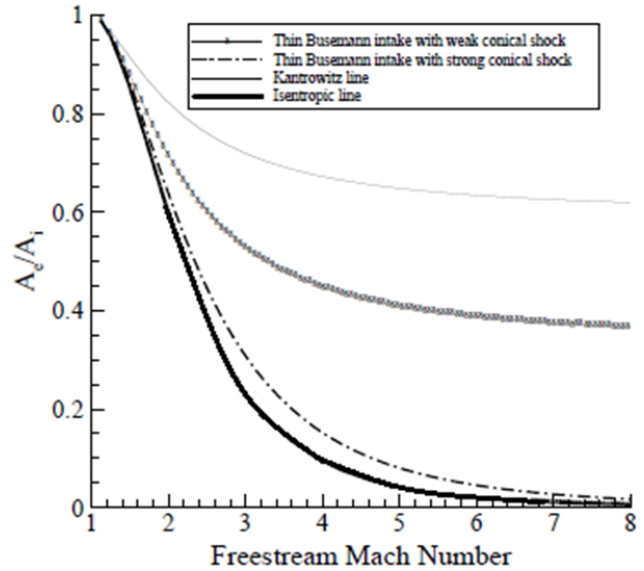

Fig. 6 Self-starting (Kantrowitz) limits for Busemann intakes

For intakes with overboard spillage, the same basic principle is used by placing a conical normal shock wave between the focal point of Busemann flow and the Busemann surface at the cross-section denoted as A_s, where the local Mach number is M_s; i.e., the normal conical shock is being placed at the entry of the enclosed section of the intake. Based on the Kantrowitz theory, if the contraction downstream of the conical normal shock does not lead to choking, then the shock would move downstream and the intake would start spontaneously. For started intake, the point (M_s, A_e/A_s) when A_e/A_s is the exit-to-entry are a ratio of the enclosed section of the intake at the Mach number of M_s, must belong to the Kantrowitz line for fully enclosed ducts.

The Busemann intake designs considered in the present study are the traditional design with a weak conical shock shown in Fig. 7 (a) and the newly produced Busemann intake design, the strong conical shock design, in which the integration of the Busemann contour begins froma strong conical shock (Fig. 7 (b)). The side views of thin Busemann intakes with weak and/or strong conical shocks are also shown in Fig. 8.

As explained before, for any combination (M_2, θ_a), the Taylor-Maccoll and streamline equations are integrated to obtain the Busemann contour and subsequently, M_∞, M_s, M_e, A_s, A_e, and A_i are calculated. If the shock angle θ_a is less than the maximum one $(\theta_a)_{max}$, the shock is weak and if $\theta_a > \theta_{max}$, there is strong conical shock. The next step is to

World Academy of Science, Engineering and Technology
International Journal of Mechanical and Mechatronics Engineering
Vol:11, No:5, 2017

compare the intake area ratio A_e/A_i with Kantrowitz value for $M = M_\infty$. If the intake area ratio satisfies the self-starting condition, $(A_e/A_i)_{Kanrowitz} \leq (A_e/A_i)$, the intake with chosen M_2 and θ_a starts spontaneously. Covering all the parametric space (M_2, θ_a), one can determine the Kantrowitz (self-starting) limit for the Busemann intakes with overboard spillage and different designs on the $(M_\infty, A_e/A_i)$ diagram, see Fig. 6.
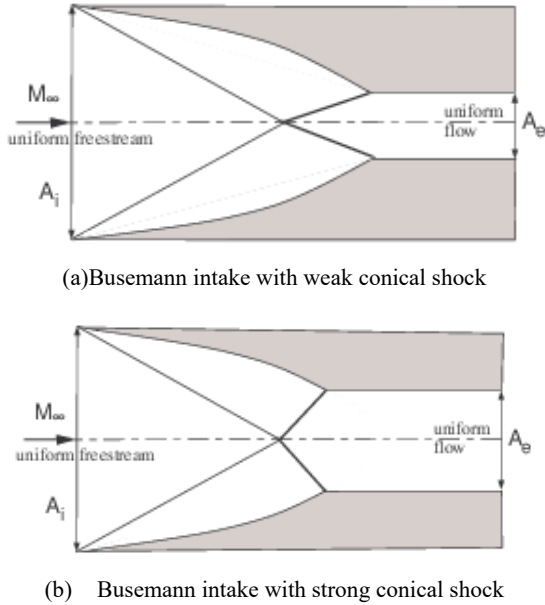

(a)Busemann intake with weak conical shock

(b)   Busemann intake with strong conical shock

Fig. 7 Busemann intake designs

(a)Weak conical shock design
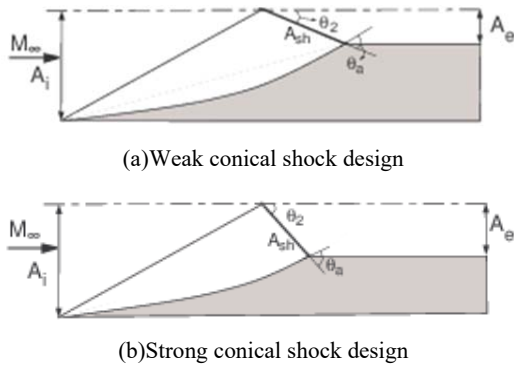

(b)Strong conical shock design

Fig. 8 Thin Busemann intake designs side views

However, it should be immediately pointed out that the above analysis is valid only in the limit $\phi \to 0$ when the overboard spillage is maximized. By increasing ϕ, the spillage sideways and eventually upwards are restricted by the Busemann surface walls and it is completely eliminated at $\phi = 360°$; thus, using modified area ratio for the internal compression section A_e/A_s for various capture angles is suggested which demonstrates the change in overboard spillage.

$$\frac{A_e}{\widetilde{A}_s} = \frac{A_e}{A_s - f(\phi)(A_s - A_i)} \tag{4}$$

where $0 \leq f(\phi) \leq 1$ is a function of the capture angle satisfying the following conditions: $f(\phi) = 0$ and $f(2\pi) = 1$. Therefore, using these conditions for $f(\phi)$, the area ratio of the fully enclosed intake $\phi = 2\pi = 360°$ is recovered A_e/A_i, and, in the case of $\phi = 0$, the non-modified area ratio A_e/A_s is used.

It would be logical to relate the function $f(\phi)$ to the magnitude of the spillage area. The function $f(\phi)$ should be equal to 1 in the absence of spillage and it will be equal to zero when spillage is maximized $(\widetilde{A}_s = A_s)$.

The function of $f(\phi)$ is defined as:

$$f(\phi) = 1 - \frac{A_{spill}/A_{(i-\phi)}}{A_{max-spill}/A_{(i-0)}} \tag{5}$$

Thus, for any Busemann intake with capture angle of ϕ, the function $f(\phi)$ is defined as the difference between 1 and the ratio of the spillage area to the maximum spillage area. The spillage areas should be normalized by the inlet area.

It is clear that for a full Busemann intake with $\phi = 360°$ and no spillage, $\left(A_{spill}/A_{(i-360°)}\right)$ is equal to zero, $f(\phi = 360°) = 1$ and, therefore, $(\widetilde{A}_s = A_i)$. On the other hand, when $\phi \to 0$ for thin Busemann intake, $(A_{spill}/A_{(i-\phi)})$ is equal to $\left(A_{max-spill}/A_{(i-0°)}\right)$, which gives $f(0°) = 0$ and $(\widetilde{A}_s = A_s)$.

The spillage area A_{spill} is given by (1), (2), or (3).Then, using the capture area $A_{(i-\phi)}$ equal to $(\phi/2)R_i^2$,

$$Theory\ I: \begin{cases} \dfrac{A_{spill-(\phi \leq 180°)}}{A_{(i-\phi \leq 180°)}} = \dfrac{\sin(\phi/2)}{(\phi/2)\tan\alpha(\tan\alpha\cos(\phi/2))} \\[3mm] \dfrac{A_{spill-(\phi \geq 180°)}}{A_{(i-\phi \geq 180°)}} = \dfrac{\sin(\phi/2)}{(\phi/2)\tan\alpha(-\tan\alpha\cos(\phi/2))} \end{cases} \tag{6}$$

$$Theory\ II: \frac{A_{spill-(\phi \leq 180°)}}{A_{(i-\phi \leq 180°)}} = \frac{A_{spill-(\phi \geq 180°)}}{A_{(i-\phi \geq 180°)}} = \frac{\sin(\phi/2)}{(\phi/2)\tan\alpha} \tag{7}$$

For a thin Busemann intake, $A_{(i-0°)}$ is equal to R_i. Thus,

$$\frac{A_{max-spill}}{A_{(i-0)}} = \begin{bmatrix} Theory\ I \\ = M_\infty \\ Theory\ II \\ = \dfrac{1}{\tan\alpha} \end{bmatrix} \tag{8}$$

Finally, when any one of the above-mentioned theories is used, $f(\phi)$ can be determined for any chosen ϕ as:

World Academy of Science, Engineering and Technology
International Journal of Mechanical and Mechatronics Engineering
Vol:11, No:5, 2017

$$\text{Theory I}:\begin{cases} f(\phi)_{(0^\circ<\phi\leq180^\circ)} = 1 - \dfrac{\cos\alpha\sin(\phi/2)}{(\phi/2)(\tan\alpha\cos(\phi/2))} \\[2mm] f(\phi)_{(180^\circ\leq\phi<360^\circ)} = 1 - \dfrac{\cos\alpha\sin(\phi/2)}{(\phi/2)(-\tan\alpha\cos(\phi/2))} \end{cases} \quad (9)$$

$$\text{Theory II}: f(\phi)_{(0^\circ<\phi\leq180^\circ)} = f(\phi)_{(180^\circ\leq\phi<360^\circ)} = 1 - \dfrac{\sin(\phi/2)}{(\phi/2)} \quad (10)$$

Fig. 9 shows $f(\phi)$ values calculated using both theories when ϕ is increasing from 0° to 360°. It is clear that as explained before, the geometric alanalysis used to find spillage area A_{spill} in Theory I and Theory II results in gradually increasing of $f(\phi)$ by increasing capture angle ϕ. It looks like the maximum slope of increasing the spillage is related to half-Busseman intakes.
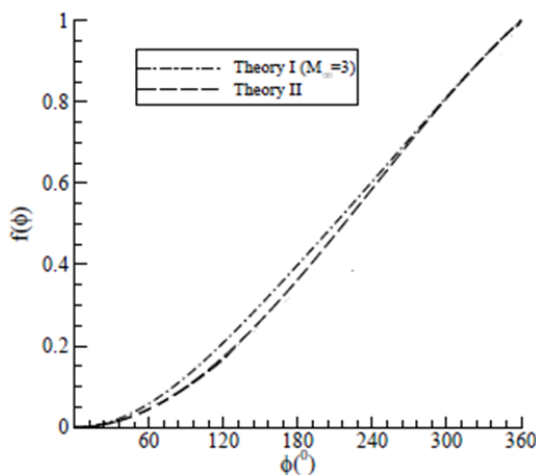

Fig. 9 Variation of $f(\phi)$ vs. ϕ

Knowing the modified area ratio at any ϕ, the startability analysis for the cases with $0^\circ<\phi<360^\circ$ starts by choosing a pair (M_2, θ_a). Then, the ratio A_e/A_s, which is obtained for any specific design and $\phi\approx0$, is modified to $A_e/\widetilde{A}_s$ using (4), (9) and (10). Having M_2 and the modified internal contraction area ratio $A_e/\widetilde{A}_s$, one obtains the corresponding new free-stream Mach number $\widetilde{M}_\infty$ and shock angle $\widetilde{\theta}$ /aerodynamic shock angle $\widetilde{\theta}_a$ (among all available data at M_2 and different θ_a for thin Busemann intakes) as well as the new Busemann contour and the Mach number $\widetilde{M}_s$ at the cross-section $\widetilde{A}_s$. As the final step, it is analyzed whether or not $\widetilde{M}_s$ and $A_e/\widetilde{A}_s$ satisfy the Kantrowitz criterion.

Covering all the parametric space (M_2, θ_a), the Kantrowitz limit for the Busemann intake with the given capture angle ϕ on the $(M_\infty, A_e/A_i)$ diagram can be determined. Such self-starting lines for Busemann intakes with weak and strong conical shock designs are shown for selected capture angles in

Figs. 10 and 11. It is clear that decreasing the capture angle and thereby increasing overboard spillage improves starting characteristics of Busemann intakes.
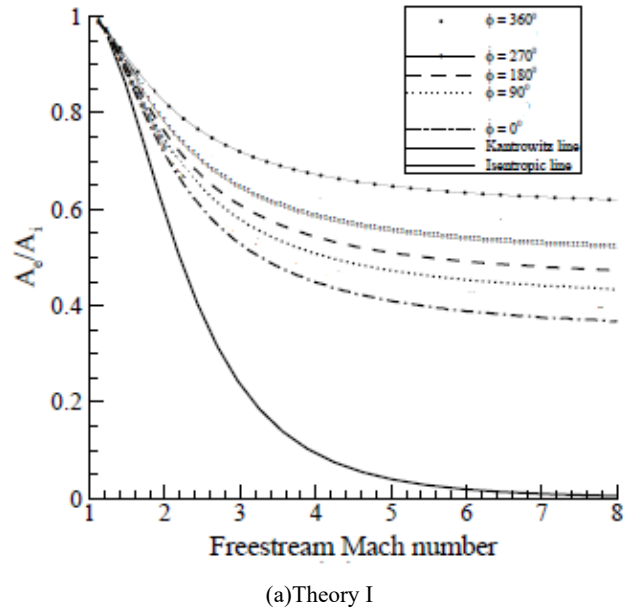
(a)Theory I
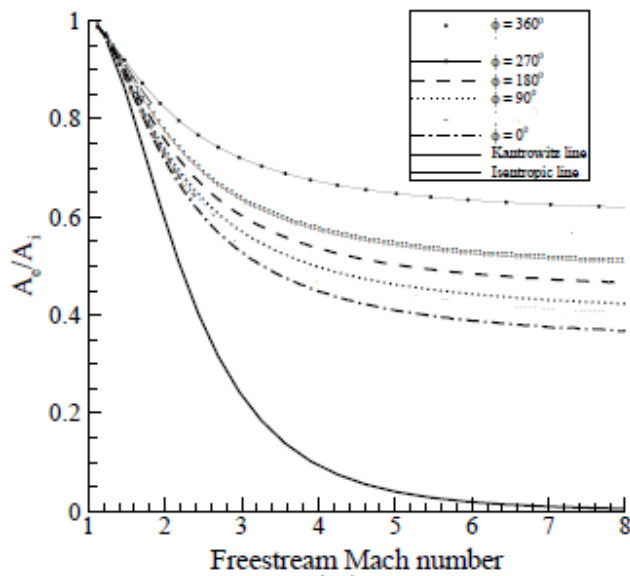
(b)   Theory II

Fig. 10 Self-starting limits of Busemann intakes with weak conical shock and different capture angles

The application of the two theories presented above results in two sets of self-starting boundaries for any chosen design of Busemann intake. As shown in Figs. 10 and 11, the results based on the second theory (Theory II) show slightly more improvement in startability via overboard spillage. These theoretical predictions of startability of Busemann intake with weak conical shock will be validated by 3D numerical starting experiments in the following section.
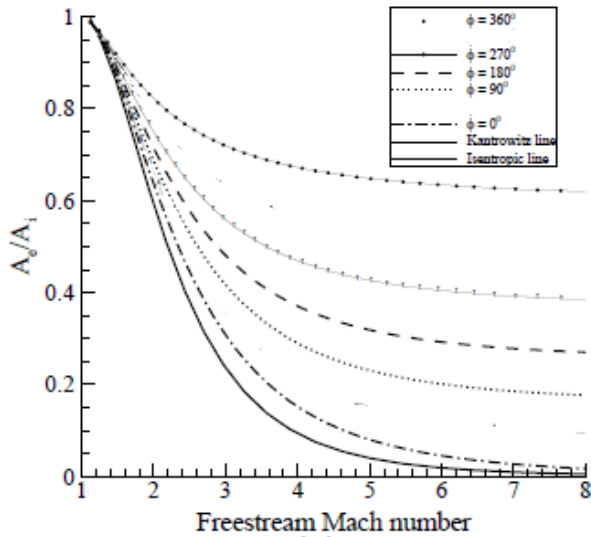
World Academy of Science, Engineering and Technology
International Journal of Mechanical and Mechatronics Engineering
Vol:11, No:5, 2017

IV. COMPUTATIONAL STARTABILITY ANALYSIS OF BUSEMANN INTAKES
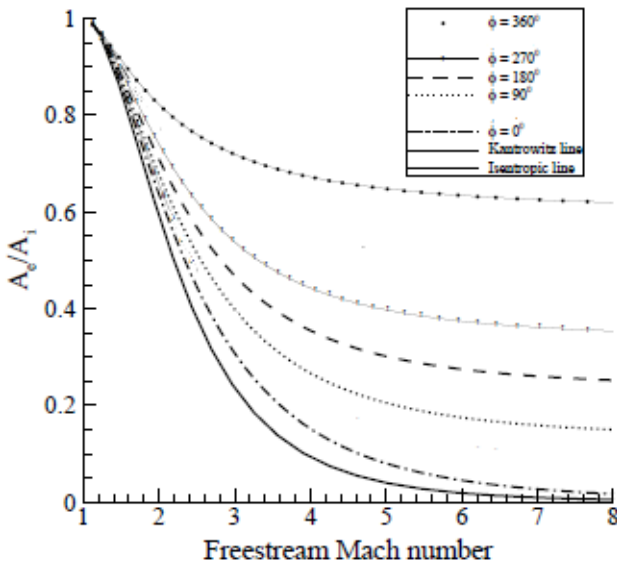
A. Numerical Model and Codes

The theoretical intake startability analysis in this study is based on the assumption of inviscid, non-heat-conducting flow of an ideal gas with constant specific heats. Accordingly, in order to numerically analyze intakes startability in quasi-steady flow, Euler finite-volume flow solvers of Masterix [23] and Candifix [24] are used.

(a)Theory I

(b)   Theory II

Fig. 11 Self-starting limits of Busemann intakes with strong conical shock and different capture angles

Numerical methods are conceptually similar to the MUSCL-Hancock method [25], [26]. In order to generate the unstructured meshes, the existing open source software, OpenCASCADE library [27], and the Netgen library [28] are

used. To achieve high resolution of localized flow features, local grid adaptation via the classical h-refinement is employed. The second order of approximation in space on smooth solutions is achieved using a linear reconstruction with a TVD limiter. The code Masterix is used for 2D simulation features build-in post-processing capabilities, while a stand-alone utility Renderix [29] is used for post processing of 3D flowfields.
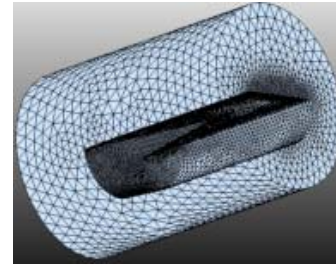

Fig. 12 The computational domain and the baseline tetrahedral mesh for 3D intake starting experiments (a half-Busemann intake)

As shown in Fig. 12, the computation domain is enclosed by a cylinder with approximate dimensions $\sim 5.8R \times \sim 4.2R$ (height vs. diameter), where R is the radius of the intake's entry cross-section $\left(A_i = \pi R^2\right)$. The unstructured mesh consists of approximately 0.5M tetrahedral cells. The smallest cells are limited to $0.001R$ while the largest cells, approaching the far-field boundaries of the computational domain, are less than $0.3R$.

In the startability analysis of all types of intakes, the free-stream properties are specified at the external boundaries of computation domains. The impermeable wall boundary condition is used on all boundaries corresponding to the intake's surfaces. At the exit of the intake, a low pressure value is specified. As initial conditions, free-stream values are usually used in the whole computational domain. It should be noted that no assumptions regarding flow symmetry of any kind or particular flow features/characteristics are made in the numerical model and the codes. Therefore, using the codes to reproduce the steady Busemann flow in the started mode can account as an additional verification.

The classical Kantrowitz theory itself and all theoretical startability considerations, taking into account overboard spillage, are based on the quasi-steady assumption; i.e., during the starting process, the free-stream velocity is assumed to vary gradually so that the starting process is considered as a sequence of steady states. To reproduce this quasi-steady condition in numerical experiments, it is necessary to increase the free-stream velocity V_∞ with sufficiently low acceleration (a) from zero to a value corresponding to chosen M_∞.

A scale analysis in the proceeding studies [30], [31] indicates that using the flow acceleration of $a \approx 100g$ is a safe assumption to reproduce quasi-steady flow. Later on, in the previous study on startability of Prandtl-Meyer intake via overboard spillage technique [12], the accuracy and the possibility of using $a = 1000g$ is confirmed. It is found that

World Academy of Science, Engineering and Technology
International Journal of Mechanical and Mechatronics Engineering
Vol:11, No:5, 2017

the starting outcome remains the same for both accelerations. Similar investigation is done in 3D analysis, and the minimum area ratios of the self-starting intakes using both accelerations are in good agreement with accuracy of 1% in terms of area ratio. Therefore, it is confirmed that there is no difference between using 100 g and 1000 g accelerations in this numerical study.

In a computationally efficient manner, the best method to satisfy the quasi-steady flow assumption which reduce the time needed for each computational run are introduced by, first, computing the unstarted steady state flowfield in the intake designed for design Mach number, e.g. $M_{design} = 4$, with the closed exit at lower free-stream Mach number, for example, $M_\infty = 3.85 < 4$. Indeed, sudden insertion of the intake into $M_\infty = 3.85$ free-stream can be used as the initial condition. Then, after achieving a steady state, the exit is suddenly opened, and the computation proceeds until a new steady state is reached. This steady state serves as the initial condition for subsequent free-stream flow acceleration towards $M_\infty = M_{design} = 4$ if the flow is unstarted. If not, an initial Mach number of $M_\infty < 3.85$ should be chosen and the process should be repeated. The accuracy of this method is verified by finding the minimum self-starting area ratios of Busemann intakes with capture angles of $180°$ and $270°$, which are designed for Mach number of 3. The area ratio of started intakes is the same as using the flow acceleration of $1000g$ from the zero velocity to design Mach number, M_{design}. Therefore, when computational time is an issue, the above method of beginning the acceleration stage, not from zero velocity but from an unstarted flow at a slightly lower Mach number can be used.

B. Self-Starting Busemann Intakes Area Ratios

The numerical simulations for the determination of the minimum self-starting area ratios of Busemann intakes with weak conical shock and provisions for overboard spillage (different capture angles) at free-stream Mach numbers 3.0, are done using unstructured adaptive Euler finite-volume flow solvers and methodology explained in the previous sections.

The Busemann contour for the intake to be tested is found by integrating the Taylor-Maccoll and streamline equations and, then imported into AutoCAD to create the 3D geometry of the computational domain, e.g. see Fig. 12. The mesh is then generated using the existing open source software [27], [28] and then, the intake starting experiment is carried out with Candifix code using the boundary conditions and methodology discussed before.

Many 3D numerical starting experiments are required to determine just one minimum self-starting area ratio for a given intake geometry, which is defined by the intake's design type and its capture angle, and free-stream Mach number. In view of all that the present study is limited to numerical starting experiments for weak-shock-based intake design (Fig. 7 (a)). The free-stream number $M_\infty = 3.0$ and 7capture angles are

considered.

The numerical computation using 2D simulation for started fully enclosed Busemann intakes $(\phi = 360°)$ results in minimum area ratios of 0.721 for started intakes at free-stream Mach numbers of 3. The results are in excellent agreement with the theoretical value of 0.71922. The minimum self-starting area ratio of thin Busemann intake $(\phi \to 0°)$ designed with weak conical shock which terminates at the trailing edge of the Busemann surface contour is found to be 0.529, which is also in good agreement with the theoretical value of 0.52845 for the self-starting boundary.

The numerical results for the minimum self-starting area ratios of the Busemann intakes designed with weak conical shock, which terminates at the trailing edge of the Busemann surface contour, and capture angles of $90°$, $135°$, $180°$, $225°$, and $270°$ at the design Mach number of 3 are shown in Fig. 13 along with the results of 2D simulations for $\phi = 0°$ and $\phi = 360°$, and the theoretical results.

It is to be noted that in Fig. 13, only the starting outcomes for the lowest started area ratio and the highest unstarted area ratio are presented. Many more experiments were conducted for each given M_∞ and ϕ; however, for clarity, these results are not included in Fig. 13.
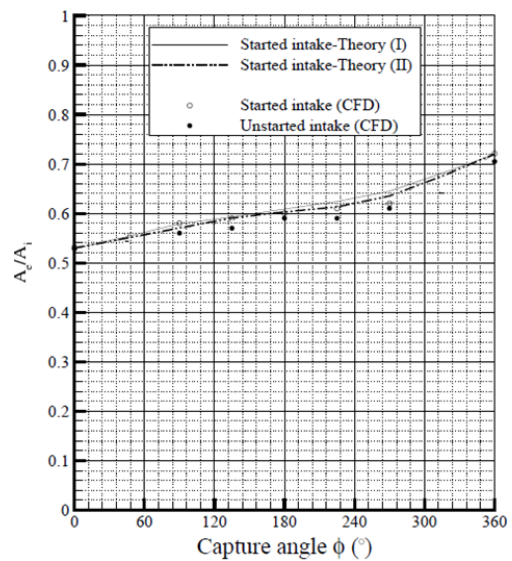

Fig. 13 Theoretical and numerical self-starting area ratios A_e/A_i vs. capture angle ϕ for Busemann intakes designed with weak conical shock for $M_\infty = 3$

Clearly, both theories qualitatively agree with the numerical results; specifically, Theory II in which only spillage is in upward direction. The numerical results show that the minimum self-starting area ratio decreases with the decrease of capture angle monotonically. However, the rate of change of the area ratio varies with capture angle. It is clear that in a range of capture angles centered at $\phi = 180°$, the minimum

World Academy of Science, Engineering and Technology
International Journal of Mechanical and Mechatronics Engineering
Vol:11, No:5, 2017

self-starting area ratio is much less sensitive to the variations of capture angle and stays nearly constant.

V. CONCLUSION

A new way to introduce overboard spillage for Busemann intakes, without altering the started flow, is suggested by considering angular sectors or portions of full Busemann intakes with different capture angles. Furthermore, in addition to the well-known Busemann intakes with a weak conical shock, a new design of Busemann intake, the strong-shock-based design, is put forward.

Two different theories based on geometrical considerations are developed to calculate the spillage amount for Busemann intakes with different capture angles. The startability analysis of different designs of Busemann intakes with overboard spillage is done using these theories. All the obtained self-starting boundaries for Busemann intakes show significant improvement in startability of the intakes via overboard spillage. Among the considered designs, the strong conical shock design results in the lowest self-starting area ratios. Therefore, the strong design principle appears to be valid in this case as well.

Considering the influence of capture angle alone on startability of Busemann intakes, one may conclude that the influence of capture angle ϕ is nonlinear: the self-starting curves for $\phi \leq 180°$ is noticeably closer to the limiting case of $\phi \approx 0$ with the highest startability rather than to the case of fully enclosed Busemann intake $\left(\phi = 360°\right)$.

The differences between the theoretical results are due to the fact that the evaluation of overboard spillage effect is based on different purely geometrical considerations. In order to validate the developed analytical treatment of self-starting boundaries, the minimum self-starting area ratios for Busemann intakes with overboard spillage are obtained via numerical starting experiments.

Generally, the outcomes of the numerical experiments on self-starting of Busemann intakes with overboard spillage confirm the theoretical predictions. It is clearly demonstrated that the startability of Busemann intakes is improved by overboard spillage. It is shown that decreasing the capture angle of Busemann intakes decreases the self-starting limiting area ratio. The second theory (Theory II) influence on intake starting demonstrates particularly good agreement with the data from numerical experiments in spite of its simplicity.

ACKNOWLEDGMENT

REFERENCES

[1] D. M. Van Wie, F. T. Kwok, and R. F. Walsh, "Starting characteristics of supersonic inlets," AIAA Paper 96-2914, *AIAA*, 1996.
[2] C. G. Rodriguez, "CFD analysis of the CIAM/NASA scramjet," AIAA 2002-4128, *AIAA*, 2002.
[3] L. Yue, L. Chen, Y.Xiao, P. Gong, and X. Chang, "Research on three-dimensional scramjet inlet," AIAA Paper 2006-9141, *AIAA*, 2006.
[4] Y. Wang, J. Liang, X. Fan, W. Liu, and Z. Wang, "Investigation on the unstarted flowfield of a three dimensional sidewall compression hypersonic inlet," AIAA Paper 2009-7404, *AIAA*, 2009.
[5] K. E. Hutchins, M. R. Akella, N. T. Clemens, and J. M. Donbar, "Detection and transient dynamics modeling of experimental hypersonic inlet unstart," AIAA 2012-2808, *AIAA*, 25-28 June 2012.
[6] A. Kantrowitz, and C. Donaldson, "Preliminary investigation of supersonic diffusers," Advance Confidential Report L5D20, *NACA*, 1945.
[7] A. Kantrowitz, "The formation and stability of normal shock waves in channel flows," Technical Note 1225, *NACA*, 1947.
[8] X. Veillard, R. Tahir, E. Timofeev, and S. Molder, "Limiting contractions for starting simple ramp-type scramjet intakes with overboard spillage," *AIAA Journal of Propulsion and Power*, vol. 24, no. 5, 2008, pp. 1042-1049.
[9] B. Sun, and K. Zhang, "Empirical equation for selfstarting limit of supersonic inlets," *Journal of Propulsion and Power Technical Notes*, vol.26, no. 4, Mar. 2010, pp. 874 -875.
[10] O. M. Hohn, and A. Gulhan, "Analysis of a three-dimensional, high pressure ratio scramjet inlet with variable internal contraction," AIAA 2012-5975, *AIAA*, 24-28 Sep. 2012.
[11] N. Moradian, and E. Timofeev, "Limiting contractions for starting Prandtl-Meyer- type scramjet inlets with overboard spillage," In: Kontis, K. (Ed.), 28th International Symposium on Shock Waves, (Manchester, UK, 17-22 July, 2011), Springer, 2012, vol. 2, pp. 307-312.
[12] N. Moradian, and E. Timofeev, "Numerical modeling of supersonic inlets with improved starting characteristics via overboard spillage," In: Proceedings of the 19th Annual Conference of the CFD Society of Canada, Montreal, Quebec, April 27-29, 2011, 6 pages.
[13] M. R. Rosli, M. Takahashi, T. Sato, T. Kojima, H. Taguchi, and Y. Maru, "Streamline tracing technique based design of elliptical-to-rectangular transitioning hypersonic inlet," AIAA-2013-2665, *AIAA*, 2013.
[14] S. Molder, and E. J. Szpiro, "Busemann inlet for hypersonic speeds," *AIAA Journal of Spacecraft and Rockets*, vol. 3, no. 8, August 1966, pp. 1303-1304.
[15] A. Busemann, "Drucke auf kegelformige spitzen bei bewegung mit uberschallgeschwindigkeit," *Ztscr.f. angew. Math. und Mech.*, vol. 9, no. 6, Dec. 1929, pp. 496-498.
[16] I. Taylor., and J. W. Maccoll, "The air pressure on a cone moving at high speeds," *Proceedings of the Royal Society of London*, vol. 139, 1933, pp. 278-311.
[17] S. Molder, "A benchmark for internal flow CFD codes," *Computational fluid dynamics Journal*, vol. 12, No. 2, 2003, p. 47.
[18] S. Molder, *Curved aerodynamic shock waves,* PhD thesis, Jan. 2012.
[19] A. Busemann, "Die achsensymmetrische kegelige uberschallstromung," *Luftfahrtforschung*, vol. 19, no. 4, 1944, pp. 137-144.
[20] D. M. Van Wie, and S. Molder, "Application of Busemann intake designs for flight at hypersonic speeds," AIAA Paper 92-1210, *AIAA*, 1992.
[21] F. S. Billig, R. A. Baurle, C-J Tam, and S. F. Wornom, "Design and analysis of streamline traced hypersonic inlets," AIAA Paper 99-4974, *AIAA*, Nov. 1999.
[22] V. Ramasubramanian, R. Sarkey, and M. Lewis, "An euler numerical study of Busemann and quasi-Busemann hypersonic inlets," AIAA-2008-66, *AIAA*, Jan 2008.
[23] Masterix, Two-dimensional, multi-block, multi-gas, adaptive, unstructured mesh, unsteady and steady-state, CFD software. Software Package, Ver. 3.40.0.3018, RBT Consultants, Toronto, ON, 2010-2013.
[24] Candifix, Three-dimensional, multi-gas, adaptive, unstructured mesh, time-accurate unsteady, CFD software. Software Package, Ver. 1.10.0065, RBT Consultants, Toronto, ON, 2010-2013.
[25] E. F. Toro, *Riemann solvers and numerical methods for fluid dynamics – A practical introduction*, Springer, 2nd edition, 1999.
[26] T. Saito, P. Voinovich, E. Timofeev, and K. Takayama, *Development and application of high-resolution adaptive numerical techniques in shock wave research center in: Godunov methods: Theory and*

World Academy of Science, Engineering and Technology
International Journal of Mechanical and Mechatronics Engineering
Vol:11, No:5, 2017

applications, Edited Review, E.F. Toro (Ed.), Kluwer Academic/Plenum Publishers, New York, USA, 2001, pp. 763-784.

[27] OpenCASCADE, Getting started, http://www.opencascade.org/org/gettingstarted/.

[28] Netgen, Installation and requisite libraries, http://sourceforge.net/apps/mediawiki/netgenmesher/index.php?title=Ins tallwindows.

[29] Renderix, One-, two-, and three-dimensional, structured and unstructured data visualization software for Windows R. Software Package, Ver. 1.1.723, RBT Consultants, Toronto, ON, 2010-2013.

[30] S. Molder, and J. M. Romeskie , "Modular hypersonic intakes with conical flow," *AGARD Conference Proceedings*, no. 30, 1968.

[31] R. Tahir, S. Molder, and E. Timofeev, "Unsteady starting of high Mach number air intakes -- A CFD Study, " AIAA Paper 2003-5191, *AIAA*, 2003.

N. Moradian is born in April 1983 in Iran. Moradian got her Bachelor degree in fluid mechanics from IUT, Isfahan, Iran in 2005. In August 2008, she graduated from University of Windsor, Windsor, ON, Canada and got her Master of Science degree in Mechanical Engineering. Moradian e earned her Ph.D. Degree in Mechanical Engineering from McGill University in February 2015.

She worked as Research Assistant and Teaching Assistance for two full years (Sep. 2006-August 2008) in University of Windsor and later on, she continues her jobs for 7 more years in McGill University (Sep. 2008-Jan. 2015). After that for about 9 months year, she worked as a researcher in Aerospace field in McGill University. Then, for one year she was in maternity absence from her job and since end of July 2016, she starts her researches on turbulence, shockwave and nanotechnology in manufacturing as an Independent Researcher. She has two journal papers on startability of supersonic intakes in preparation process to submit to AIAA journals, now. She has several presentations in AIAA and ISSW conferences. She published several Journal paper about "the effects of freestream turbulence on drag coefficient of a solid sphere," in wind structure journal, Experimental thermal and fluid science journal, etc.

Dr. Moradian is a member of AIAA (American Institute of Aeronautics and Astronautics), ASHRAE (American Society of Heating, Refrigerating and Air-conditioning Engineers), and ASME (The American Society of Mechanical Engineers): Member (1992-present). She got several awards during her education including the best student poster award at ISSW29, Selected for poster presentation in McGill Engineering Research Showcase (MERS), McGill Engineering Doctoral Award (MEDA) from McGill University, McGill International Doctoral Awards (MIDAs), Educational scholarship from Univ. of Windsor, Canada, etc.